Lodz University of Technology
Department of Automation, Biomechanics and Mechatronics

Open Scientific Lectures, K11

Analytical, and numerical observation of isolated branches of periodic orbits in 1DOF & 2DOF mechanical parametric oscillator with dry friction

Presenter: M. Junaid-U-Rehman

Supervisor: Prof. Grzegorz Kudra

20, May 2025

Model description

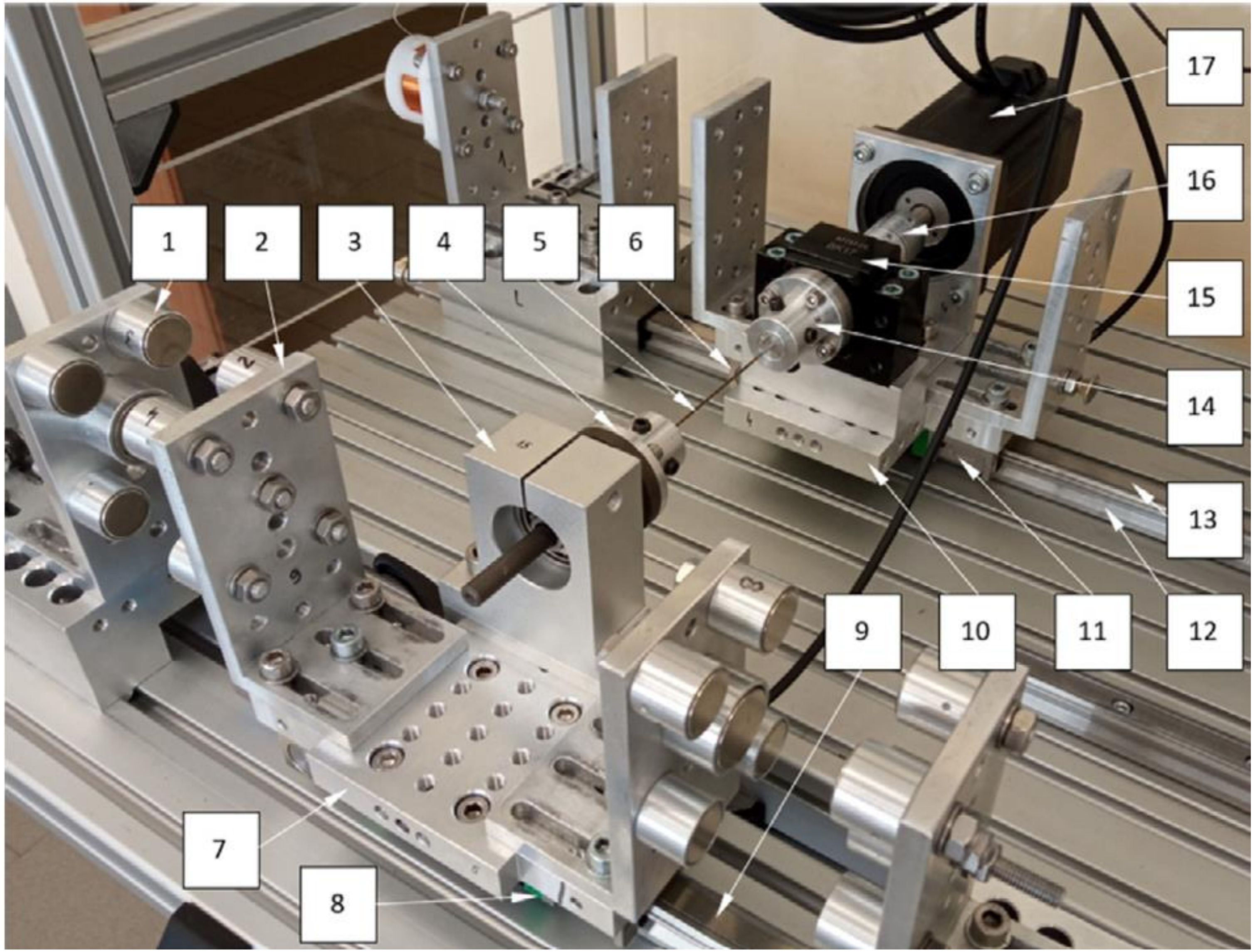

1. neodymium magnets,
2. clamps for magnets,
3. movable bearing block,
4. movable clamp of the flexible beam,
5. flexible beam,
6. manual brakes,
7. movable cart,
8. Hall sensor of the movable cart,
9. profile rail with magnetic tape,
10. fixed cart,
11. Hall sensor of the fixed cart,
12. profile rail,
13. magnetic ruler,
14. fixed clamp of the flexible beam,
15. fixed bearing block,
16. flexible clutch,
17. stepper motor with built-in encoder

Fig. 1. One degree of freedom mechanical parametric oscillator (Lab view)

Mathematical model:

Dimensional equation of the system

Assuming that all of the components are ideal, the system can be described by a second-order ODE as follows:

$$m\ddot{x} + c\dot{x} + T\frac{\dot{x}}{\sqrt{\dot{x}^2+\varepsilon^2}} + \left[\frac{k_\xi + k_\eta}{2} + \frac{k_\xi - k_\eta}{2}\cos(2\Omega t)\right]x + F_{M0}\left[\frac{1}{[1+d(\delta - x)]^4} - \frac{1}{[1+d(\delta + x)]^4}\right] = 0. \quad (1)$$

Non-Dimensional equation of the system

Define a non-dimensional time $\tau = \omega_n \cdot t$, and the non-dimensional displacement of the system as $y=\frac{x}{(\delta)}$:

$$y'' + 2\zeta y' + \sigma\frac{y'}{\sqrt{y'^2+\epsilon^2}} + [p + q\cos(2\omega\tau)]y + f_{m0}\left[\frac{1}{[1+D(1-y)]^4} - \frac{1}{[1+D(1+y)]^4}\right] = 0. \quad (2)$$

By restricting the magnetic stiffness to the 3rd term and expanding it into the Maclaurin series in Eq. (2), we get

$$y'' + 2\zeta y' + \sigma f(y') + [1 + q\cos(2\omega\tau)]y + \kappa_3 y^3 + \kappa_5 y^5 = 0. \quad (3)$$

The dry friction function $f_0(y') = \frac{y'}{\sqrt{y'^2+\epsilon^2}}$, is defined in accordance with the coulomb law, as follows;

$$f_0(y')\begin{cases} = 1, & \text{if} \quad y' > 0, \quad \text{(a)} \\ \in [-1, 1], & \text{if} \quad y' = 0, \quad \text{(b)} \\ = -1, & \text{if} \quad y' < 0. \quad \text{(c)} \end{cases} \quad (4)$$

Table.1: The parameters involved in the dimensional and non-dimensional equations (1) and (3)

Parameter	Value	Unit	Parameter	Value	Unit
F_{M0}	400.96	N	d	46.628	m^{-4}
σ	0.0096264	kg	T	1.5117	N
δ	0.02	m	ε	$1.54 \cdot 10^{-4}$	m/s
k_{ξ}	271	N/m	c	16.4754	N.s/m
k_{η}	4336	N/m	f_{M0}	2.5532	-
D	0.93255		ζ	0.043576	-
κ_1	0.70664	-	κ_3	0.82272	-
p	0.29336	-	q	0.25885	-

Department of Automation,
Biomechanics and Mechatronics

Analytical solutions

Solutions of the Eq. (3) by MMS

Here, MMS is used, and Eq. (3) becomes

$$y'' + 2\epsilon\zeta y' + \sigma\epsilon f(y') + [1 + q\epsilon\cos(2\omega\tau)]y + \epsilon\kappa_3 y^3 + \epsilon\kappa_5 y^5 = 0, \quad (5)$$

where ϵ is a small parameter. Defining the three-time variables $T_0 = \tau$ (fast time), $T_1 = \epsilon\tau$ (slow time).

The first order two-time scale expansion

The general solution of Eq. (5) can be written as;

$$y(\tau, \varepsilon) = y_0(T_0, T_1) + \epsilon\, y_1(T_0, T_1) + O(\epsilon^2). \quad (6)$$

Collecting the like powers of ϵ and equating it to zero, then we will get the set of equations. Solving the first equation for y_0

$$y_0 = A(T_1)\, e^{iT_0} + \bar{A}(T_1)\, e^{-iT_0}. \quad (7)$$

To finding the y_1, we will equate the coefficients of first power of ϵ to zero and using Eq. (7) also, we will get

$$D_0^2 y_1 + y_1 = -\kappa_5 A^5 e^{5iT_0} - (5 A^4 \bar{A} \kappa_5 + \kappa_3 A^3)\, e^{3iT_0} + [-10 A^3 \bar{A}^2 \kappa_5 - 3\kappa_3 A^2 \bar{A} - 2i D_1 A - 2i\zeta A]\, e^{iT_0} - \frac{q}{2}[A\, e^{i(2\omega+1)T_0} + \bar{A}\, e^{i(2\omega-1)T_0}] - \sigma f_0(i A\, e^{iT_0} - i \bar{A}\, e^{-iT_0}) + cc. \quad (8)$$

Further we have to evaluate the implicit terms in f_0 and we also introduce detuning parameter

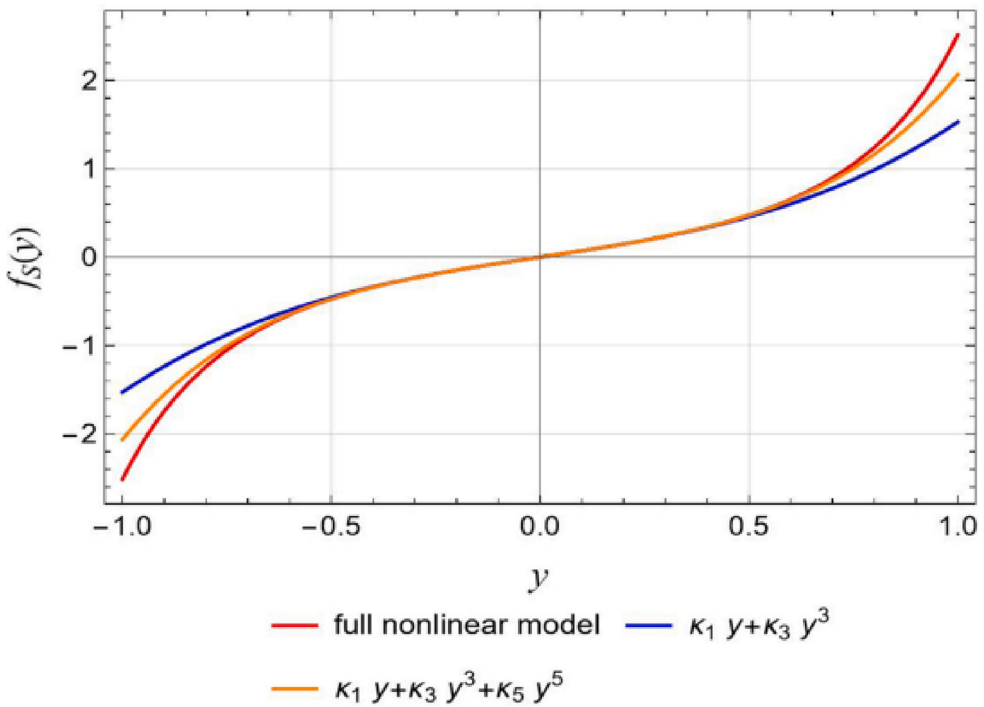

Fig. 2. Stiffness characteristics for full nonlinear model and its approximation by a 3rd and 5th degree polynomial

$\omega = 1 + \epsilon\frac{\sigma}{2}$, using it into (8), and the resonant terms in the resulting equation must disappear in order to remove secular terms, providing the solvability condition

$$-10A^3\bar{A}^2\kappa_5 - 3\kappa_3 A^2\bar{A} - 2iD_1A - 2i\zeta A - \frac{q}{2}\bar{A}e^{i\sigma T_1} - \sigma c_1 = 0. \quad (9)$$

The real and imaginary components of the solvability condition are then separated using the polar form $A = \frac{1}{2}a_{ms}e^{i\beta}$, making the system autonomous by using $\Psi = \frac{\sigma}{2}T_1 - \beta$, and after some calculation by using Maple, finally we get the 10th degree polynomial:

$$\frac{25}{256}a_{ms}^{10}\kappa_5^2 + \frac{15}{64}a_{ms}^8\kappa_5\kappa_3 + \left(\frac{9}{64}\kappa_3^2 - \frac{5}{16}q\kappa_5\right)a_{ms}^6 - \frac{3}{8}q\,a_{ms}^4\kappa_3 + \left(\frac{1}{4}\sigma^2 - \frac{1}{16}q^2 + \zeta^2\right)a_{ms}^2 + \frac{4}{\pi}\zeta\sigma a_{ms} + \frac{4}{\pi^2}\sigma^2 = 0. \quad (10)$$

The solution for Ψ is as follows: $$\Psi = \frac{1}{2}\tan^{-1}\left(\frac{-2\zeta a_{ms} - \frac{4}{\pi}\sigma}{\sigma a_{ms} - \frac{5}{8}a_{ms}^5\kappa_5 + \frac{3}{4}a_{ms}^3\kappa_3}\right). \quad (11)$$

Solutions of the Eq. (3) by HBM

Here, Using the HBM, the Eq. (3) is reformulated by applying a Fourier series formalism of the angular displacement, considering only a single harmonic below

$$y(\tau) = a_{ms}\cos\phi(\tau),\ \phi(\tau) = \omega\tau + \beta, \quad (12)$$

where a_{ms} is the amplitude, and the phase is represented by β. The dry friction phase is extended as well, employing a single-term Fourier series of the form

$$\begin{cases} f_0(y') = f_c\cos(\phi) + f_s\sin(\phi), \\ \quad\quad\;\; = f_c\cos(\omega\tau) + f_c\sin(\omega\tau). \end{cases} \quad (13)$$

where f_c and f_s are the coefficients of the expansion, using (12), (13) into (3):

$$[\sigma f_s - 2a_{ms}\omega\zeta + \frac{1}{2} q a_{ms}\sin(2\beta)]\sin(\phi) + [a_{ms} + \sigma f_c - a_{ms}\omega^2 + \frac{1}{2} q\, a_{ms}\cos(2\beta) + \frac{3}{4}\kappa_3\, a_{ms}^3 + \frac{5}{4}\kappa_5\, a_{ms}^5]\cos(\phi) = 0, \quad (14)$$

Where the coefficients of the expansion f_c and f_s are read as follows

$$\begin{cases} f_c = 0, \\ f_s = \dfrac{-4}{\pi}, \end{cases} \Rightarrow \begin{cases} -2a_{ms}\,\omega\,\zeta - \dfrac{4}{\pi}\sigma + \dfrac{1}{2} q\, a_{ms}\sin(2\beta) = 0, \\ a_{ms} - a_{ms}\omega^2 + \dfrac{1}{2} q\, a_{ms}\cos(2\beta) + \dfrac{3}{4}\kappa_3\, a_{ms}^3 + \dfrac{5}{8}\kappa_5\, a_{ms}^5 = 0. \end{cases} \quad (15)$$

We noticed that $a = 0$ is a trivial case, and it is not a solution to the above system. Squaring and adding the Eq. (15) to eliminate the 2β, we obtain

$$\frac{25}{64} a_{ms}^{10}\kappa_5^2 + \frac{15}{16} a_{ms}^8\kappa_5\kappa_3 + (\frac{9}{16}\kappa_3^2 - \frac{5}{4}\omega^2\kappa_5 + \frac{5}{4}\kappa_5)a_{ms}^6 + \frac{3}{2}\kappa_3(1-\omega^2)a_{ms}^4 + (1+\omega^4 - 2\omega^2 + 4\omega^2\zeta^2 - \frac{1}{4}q^2)\, a_{ms}^2 + \frac{16}{\pi}\omega\sigma\zeta\, a_{ms} + \frac{16}{\pi^2}\sigma^2 = 0. \quad (16)$$

From Eq. (15), we can write

$$\beta = \frac{1}{2}\tan^{-1}\left(\frac{2\zeta\omega\, a_{ms} + \frac{4}{\pi}\sigma}{a_{ms}\omega^2 - a_{ms} - \frac{3}{4}a_{ms}^3\kappa_3 - \frac{5}{8}a_{ms}^5\kappa_5}\right). \quad (17)$$

Discussion and graphics of obtained results

Department of Automation,
Biomechanics and Mechatronics

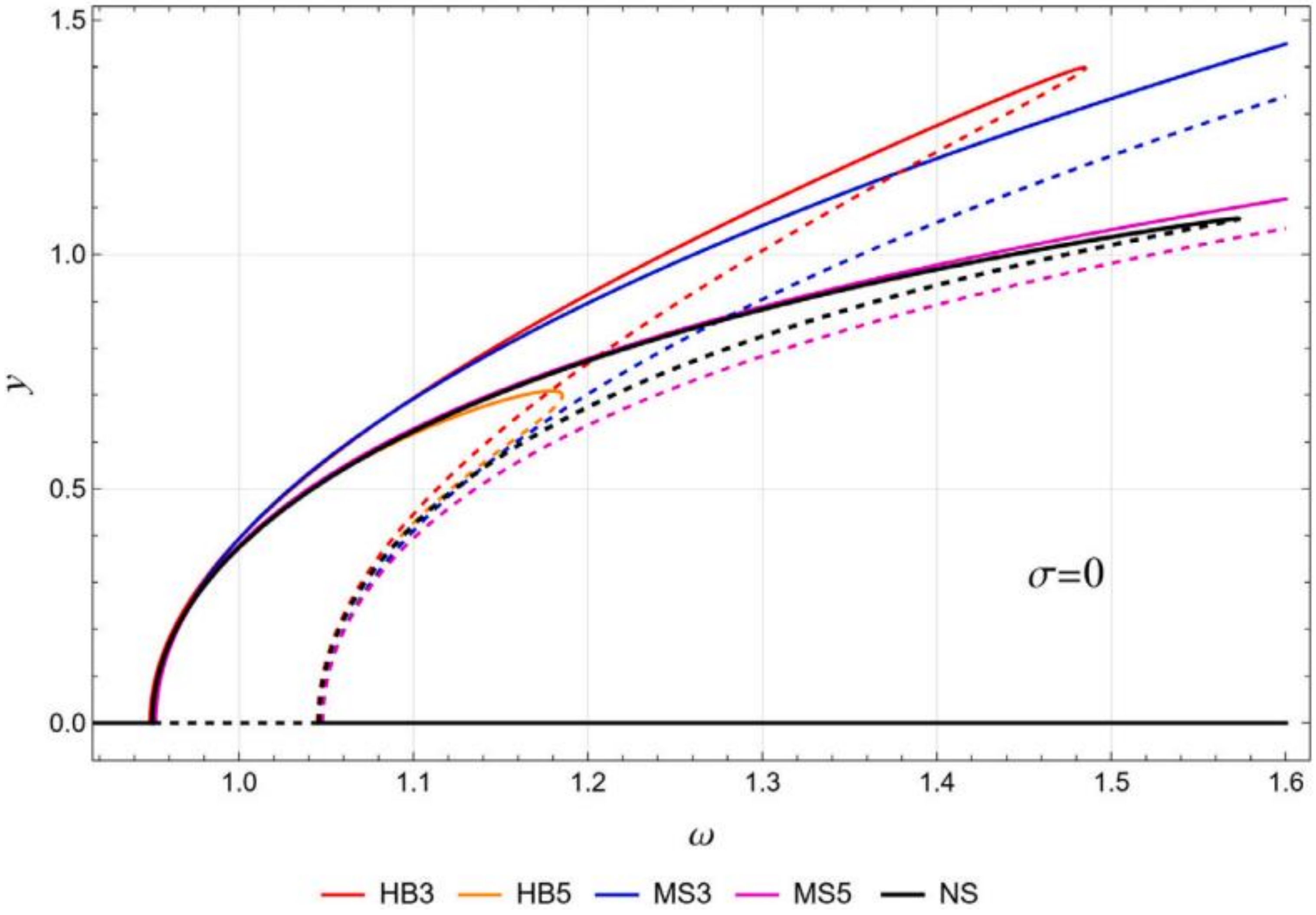

Fig.5: Branches of trivial solutions and periodic orbits (amplitudes), for $\sigma = 0$, obtained using different analytical approaches: harmonic balance method for stiffness characteristics described by a 3rd (HB3) and 5th-degree polynomial (HB5), multiple scale method for stiffness characteristics described by a 3rd (MS3) and 5th-degree polynomial (MS5), compared to the numerical solution.

Discussion and graphics of obtained results

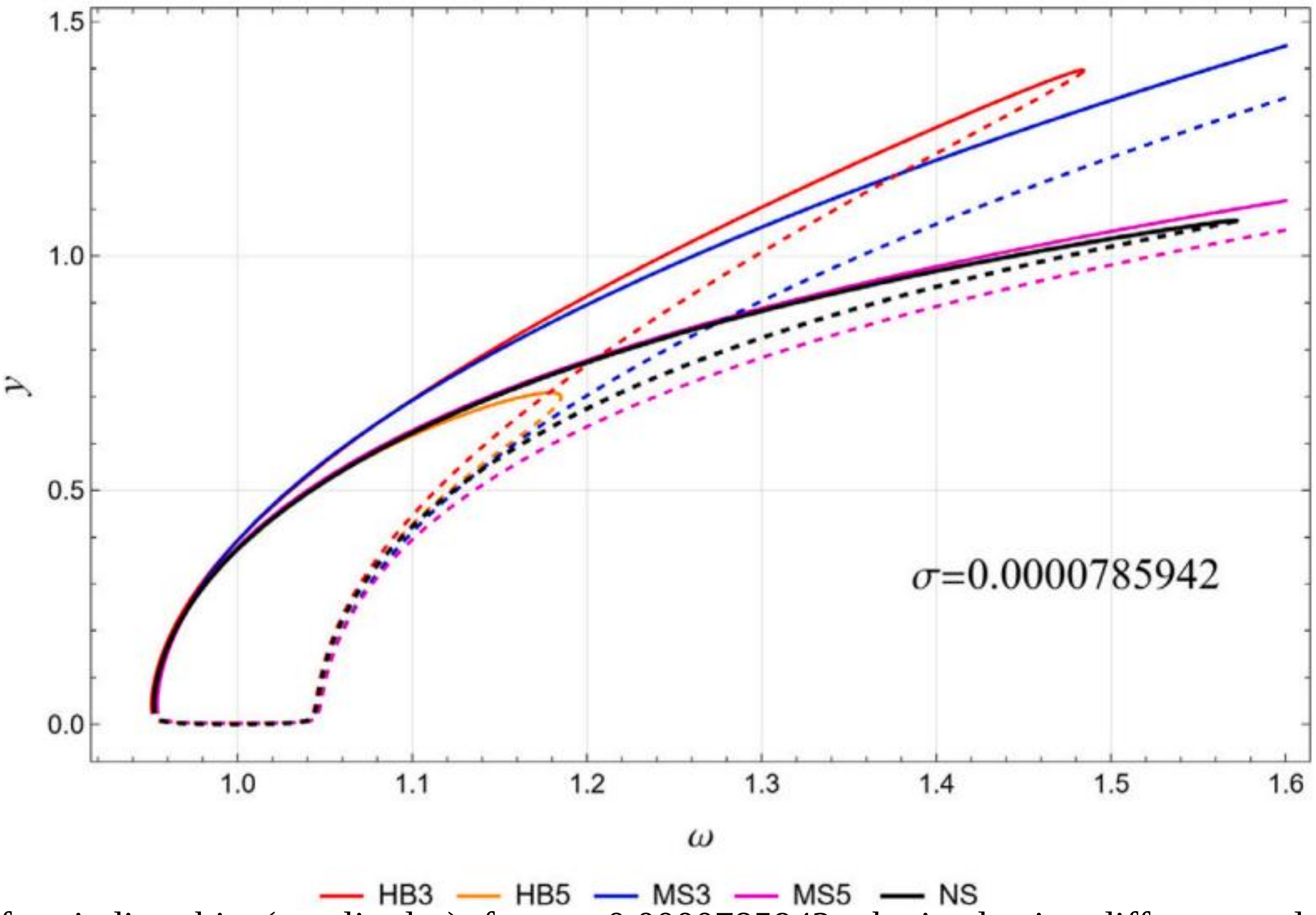

Fig.6: Branches of periodic orbits (amplitudes), for σ = 0.0000785942, obtained using different analytical approaches: harmonic balance method for stiffness characteristics described by a 3rd (HB3) and 5th-degree polynomial (HB5), multiple scale method for stiffness characteristics described by a 3rd (MS3) and 5th-degree polynomial (MS5), compared to the numerical solution.

Discussion and graphics of obtained results

Department of Automation,
Biomechanics and Mechatronics

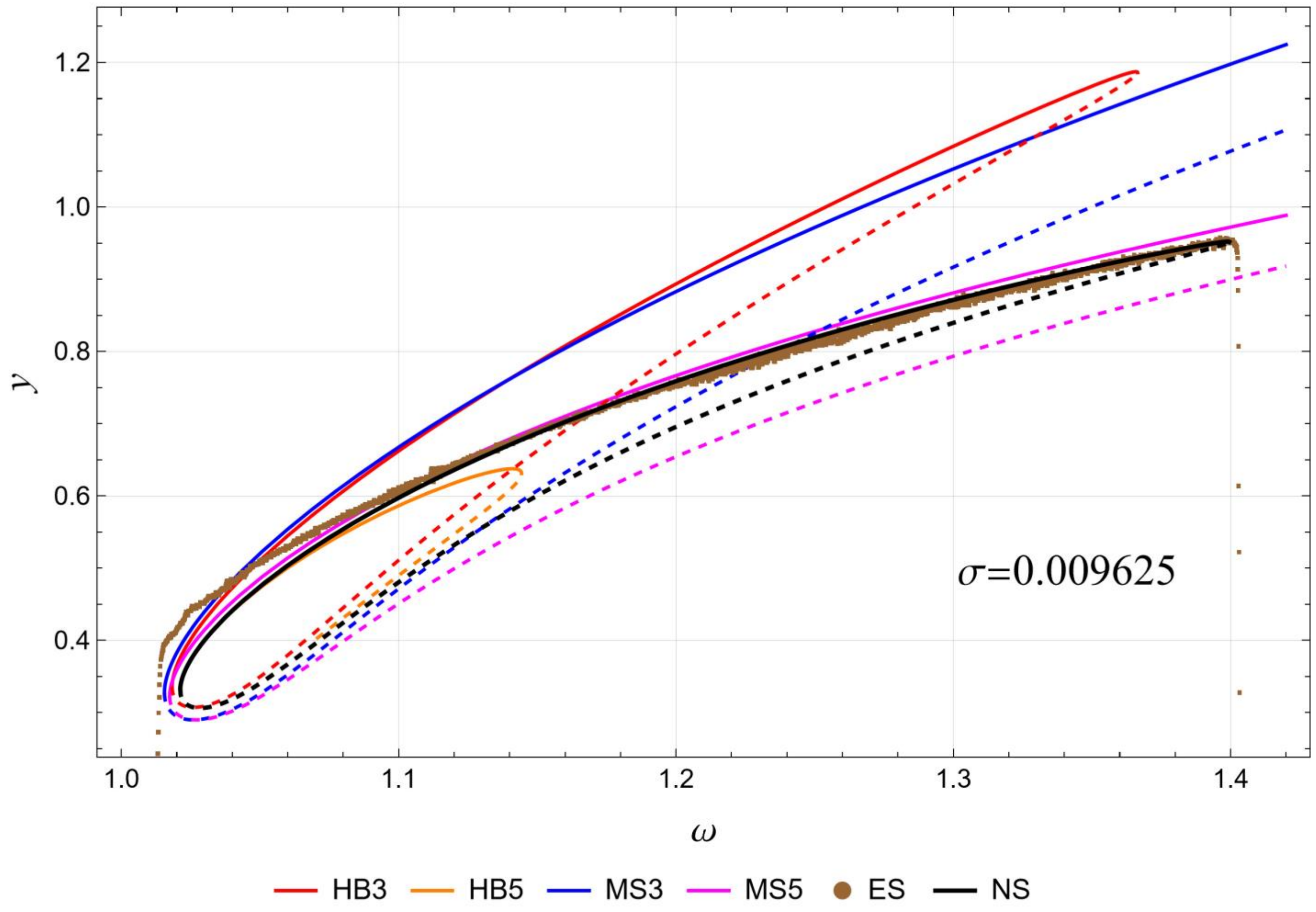

Fig.7: Branches of periodic orbits (amplitudes), for σ = 0.009625, obtained using different analytical approaches: harmonic balance method for stiffness characteristics described by a 3rd (HB3) and 5th-degree polynomial (HB5), multiple scale method for stiffness characteristics described by a 3rd (MS3) and 5th-degree polynomial (MS5), compared to experimental results (ES) and the numerical solution (NS).

Continuation of earlier published work

Dimensional equations of motion for 2DOF system

A set of 2nd order coupled ordinary differential equations of the supposed system can be written as

$$m_1\ddot{x} + c_1\dot{x} + T_1\mathrm{sign}(\dot{x}) + K(t)(x-y) + F_{s1}(x) = 0, \tag{18a}$$

$$m_2\ddot{y} + c_2\dot{y} + T_2\mathrm{sign}(\dot{y}) + K(t)(y-x) + F_{s2}(y) = 0. \tag{18b}$$

Here we try to use the following model of magnetic springs

$$F_{si}(x_i) = k_{i1}x_i + k_{i3}x_i^3 + \cdots + k_{in}x_i^n. \tag{19}$$

Non-Dimensional equations of motion for 2DOF system

By converting Eqs. (1a) & (1b) into non-dimensional form, we may establish a non-dimensional time variable, $\tau = \omega_n t$, and non-dimensional displacement of the system $u_i = \frac{x_i}{\delta}$, where $(x_1, x_2) = (x, y)$ and $(u_1, u_2) = (u, v)$, using these assumptions and we have:

$$u'' + 2\zeta_1 u' + \sigma_1\mathrm{sign}(u') + \big(p + q\cos(2\omega\tau)\big)(u-v) + (1-p)u + \kappa_{13}u^3 + \cdots + \kappa_{1n}u^n = 0, \tag{20a}$$

$$v'' + 2\zeta_2 v' + \sigma_2\mathrm{sign}(v') + \mu\big(p + q\cos(2\omega\tau)\big)(u-v) + \kappa_{21}v + \kappa_{23}v^3 + \cdots + \kappa_{2n}v^n = 0. \tag{20b}$$

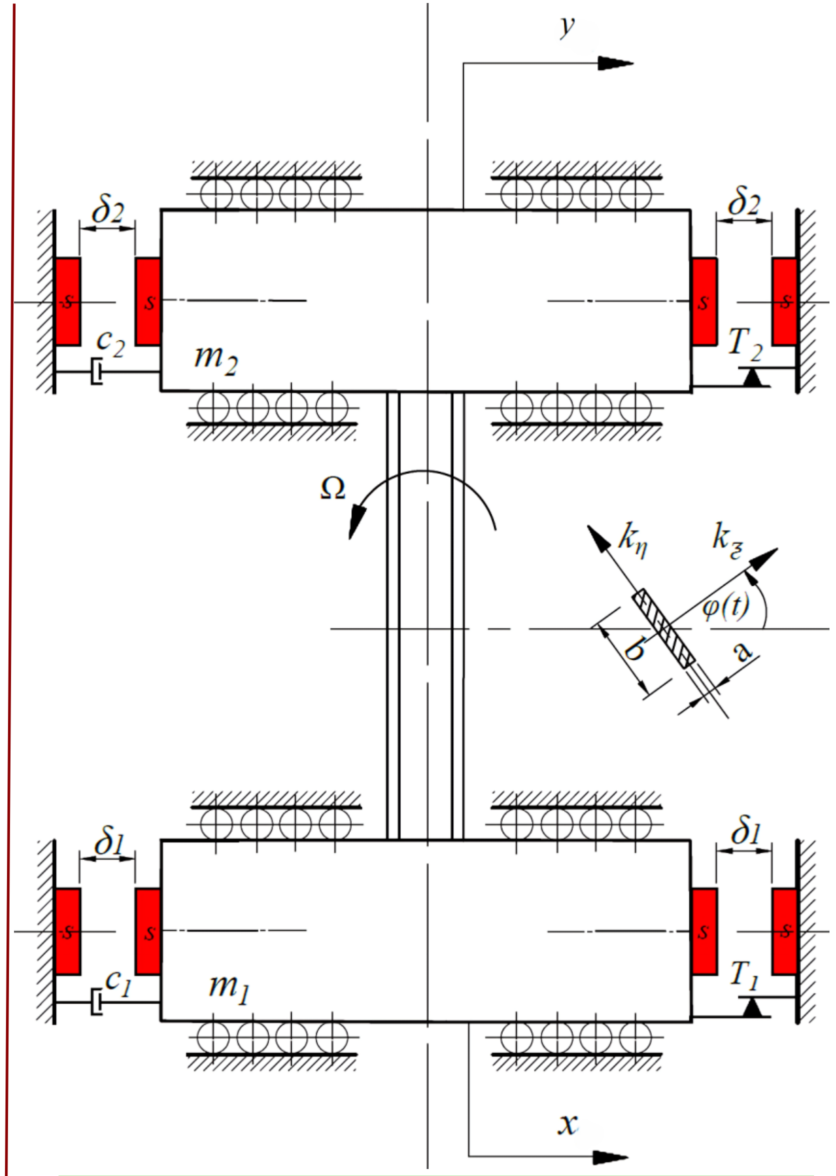

Fig. 8. 2DOF mechanical parametric oscillator

Where,

$$\zeta_i = \frac{c_i}{2m_i\omega_n}, \quad \sigma_i = \frac{T_i}{m_i\,\omega_n^2\delta_1}, \quad p = \frac{k_\xi + k_\eta}{2m_1\omega_n^2}, \; q = \frac{k_\xi - k_\eta}{2m_1\omega_n^2}\;, \kappa_{ij} = \frac{\delta_1^{j-1}}{m_i\omega_n^2}k_{ij}, \mu = \frac{m_1}{m_2}.$$

Case 1:

$$u" + 2\zeta_1 u' + \sigma_1 \mathrm{sign}(u') + \big(p + q\cos(2\omega\tau)\big)(u - v) + (1 - p)u + \kappa_{13}u^3 = 0, u_i' > 0 \quad (21a)$$

$$v" + 2\zeta_2 v' + \sigma_2 \mathrm{sign}(v') + \mu\big(p + q\cos(2\omega\tau)\big)(u - v) + \kappa_{21}v + \kappa_{23}v^3 = 0. \quad (21b)$$

Case 2:

$$u" + 2\zeta_1 u' + \sigma_1 \mathrm{sign}(u') + \big(p + q\cos(2\omega\tau)\big)(u - v) + (1 - p)u + \kappa_{13}u^3 + \kappa_{15}u^5 = 0, \quad (22a)$$

$$v" + 2\zeta_2 v' + \sigma_2 \mathrm{sign}(v') + \mu\big(p + q\cos(2\omega\tau)\big)(u - v) + \kappa_{21}v + \kappa_{23}v^3 + \kappa_{25}v^5 = 0. \quad (22b)$$

$$f_0(u_i') \begin{cases} = 1, & \text{if} \quad u_i' > 0, \quad \text{(a)} \\ \in [-1, 1], & \text{if} \quad u_i' = 0, \quad \text{(b)} \\ = -1, & \text{if} \quad u_i' < 0. \quad \text{(c)} \end{cases}$$

Where, $(u_1, u_2) = (u, v)$.

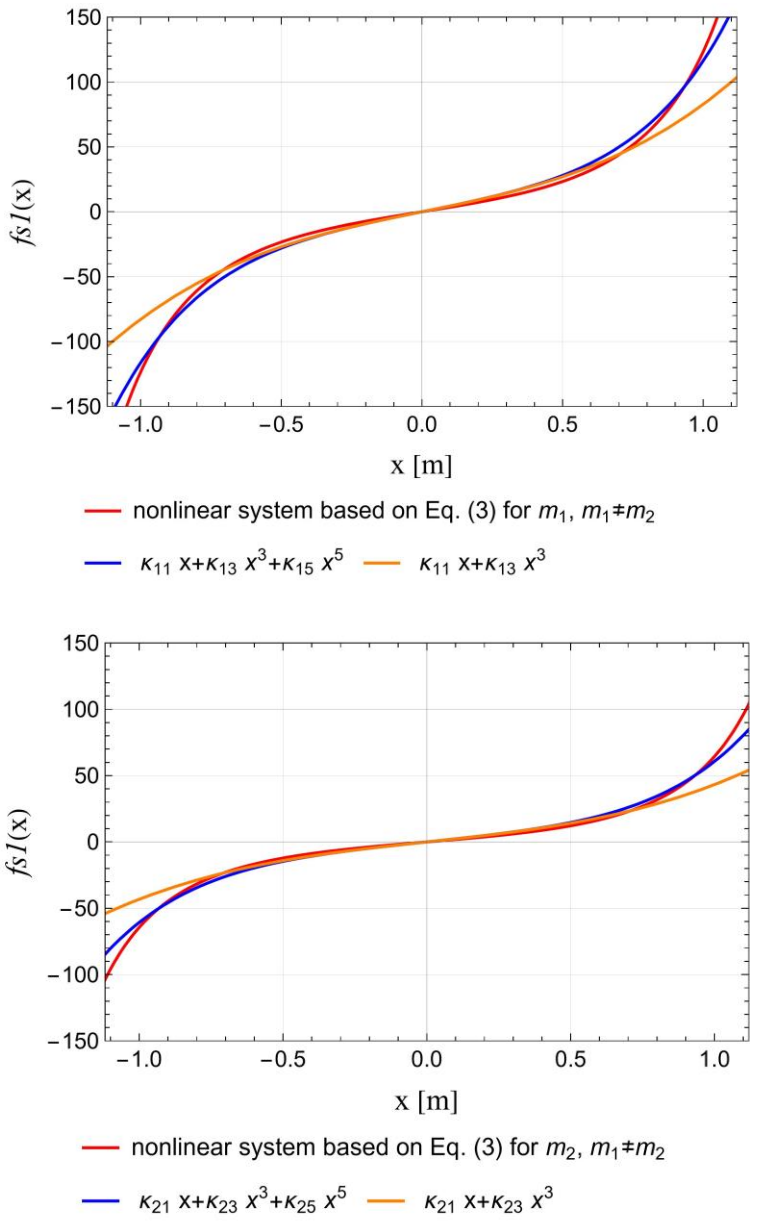

Fig. 9: Nonlinear system based on Eq. (3) and its approximation using a 3rd and 5th-degree polynomial

Department of Automation,
Biomechanics and Mechatronics

Table.2: Parameters identified on the real experimental stand

Parameter	Value	Unit	Parameter	Value	Unit
F_{M01}	400.96	N	d_1	46.628	m^{-4}
μ	m_2/m_1	kg	T_1	1.5117	N
δ_1	0.02	m	T_2	T_1	N
k_ξ	4335.9463	N/m	c_1	16.4754	N.s/m
k_η	270.9966	N/m	c_2	c_1	N.s/m

Table.3: The parameters involved in the dimensional and non-dimensional systems (18) and (21) for the same masses for n=3

Parameter	Value	Unit	Parameter	Value	Unit
m_1	4.55	kg	ζ_1	46.628	m^{-4}
m_2	4.55	kg	ζ_2	1.5117	-
σ_1	0.0134	m	σ_2	0.0134	-
κ_{11}	0.5905	N/m	κ_{21}	0.5905	-
κ_{13}	2.6736	N/m	κ_{23}	2.6736	-
μ	1	-	ω_n	35.1567	Rad/s

Table. 4: The parameters involved in the system (18) and (21) for the different masses for n=3

Parameter	Value	Unit	Parameter	Value	Unit
m_1	4.55	kg	ω_n	35.1567	rad/s
m_2	8.72	kg	ζ_1	0.0515	-
μ	1.9165	-	ζ_2	0.0268	-
σ_1	0.0134	-	σ_2	0.0070	-
κ_{11}	0.5905	-	κ_{21}	0.3082	-
κ_{13}	2.6736	-	κ_{23}	1.3954	-

Table. 5: The parameters involved in the system (18) and (22) for the same masses for n=5

Parameter	Value	Unit	Parameter	Value	Unit
m_1	4.55	kg	ω_n	42.7057	rad/s
m_2	4.55	kg	ζ_1	0.0424	-
σ_1	0.0091	-	ζ_2	0.0424	-
σ_2	0.0091	-	μ	1	-
κ_{11}	0.7225	-	κ_{21}	0.7225	-
κ_{13}	0.3430	-	κ_{23}	0.3430	-
κ_{15}	1.2910	-	κ_{25}	1.2910	-

Table. 6: The parameters involved in the system (18) and (22) for the different masses for n=5

Parameter	Value	Unit	Parameter	Value	Unit
m_1	4.55	kg	ω_n	42.7057	rad/s
m_2	8.72	kg	ζ_1	0.0423	-
σ_1	0.0091	-	ζ_2	0.0221	-
σ_2	0.0047	-	μ	1.9165	-
κ_{11}	0.7224	-	κ_{21}	0.3771	-
κ_{13}	0.3429	-	κ_{23}	0.1790	-
κ_{15}	1.2910	-	κ_{25}	0.6738	-

Complex Averaging Method

To derive the amplitude-frequency response, the CA method is employed. Following that, the amplitude modulations are averaged throughout a single period of the specified vibration frequency. Let $A_1, A_2 \in \mathbb{C}$

$$2A_1(\tau)e^{i\omega\tau} = u(\tau) - i\frac{u'(\tau)}{\omega}, \qquad 2A_2(\tau)e^{i\omega\tau} = v(\tau) - i\frac{v'(\tau)}{\omega}. \tag{23}$$

Using Eq. (23), we can write the expressions for $u(\tau)$, $u'(\tau)$, $u''(\tau)$, $v(\tau)$, $v'(\tau)$, *and* $v''(\tau)$ of the form below

$$u = A_1e^{i\omega\tau} + \overline{A_1}e^{-i\omega\tau}, \qquad v = A_2e^{i\omega\tau} + \overline{A_2}e^{-i\omega\tau}, \tag{24a}$$

$$u' = i\omega\left(A_1e^{i\omega\tau} - \overline{A_1}e^{-i\omega\tau}\right), \qquad v' = i\omega\left(A_2e^{i\omega\tau} - \overline{A_2}e^{-i\omega\tau}\right), \tag{24b}$$

$$u'' = 2i\omega A_1'e^{i\omega\tau} - \omega^2 u, \qquad v'' = 2i\omega A_2'e^{i\omega\tau} - \omega^2 v. \tag{24c}$$

Substituting the Eq. (24) into Eq. (22), we get the following simplified form:

$$\begin{cases} 2\zeta_1\omega A_1 + 2i\omega A_1' + A_1 - pA_2 + \sigma_1 f_0 + \frac{q}{2}\left(\overline{A_1} - \overline{A_2}\right) + 3\kappa_{13}A_1^2\overline{A_1} + 10\kappa_{15}A_1^3\overline{A_1^2} - \omega^2 A_1 = 0, \\ 2i\zeta_2\omega A_2 + 2i\omega A_2' + \kappa_{21}A_2 - \mu pA_1 + \mu pA_2 + \sigma_2 g_0 + \frac{\mu q}{2}\left(\overline{A_2} - \overline{A_1}\right) + 3\kappa_{23}A_2^2\overline{A_2} + 10\kappa_{25}A_2^3\overline{A_2^2} - \omega^2 A_2 = 0 \end{cases} \tag{25}$$

Using the polar form $A_1 = \frac{1}{2}a_1e^{i\alpha_1}$, $A_2 = \frac{1}{2}a_2e^{i\alpha_2}$ into Eq. (25), and supposing $A_1' = A_2' = 0$, for steady case;

$$\frac{5}{8}\kappa_{15}a_1^5+\frac{3}{4}\kappa_{13}a_1^3-pa_2e^{i(\alpha_2-\alpha_1)}-\frac{q}{2}a_2e^{-i(\alpha_2+\alpha_1)}+\frac{q}{2}a_1e^{-2i\alpha_1}+2i\zeta_1\omega a_1-\omega^2a_1+a_1+\frac{4i\sigma_1}{\pi}=0, \tag{26a}$$

$$\frac{5}{8}\kappa_{25}a_2^5+\frac{3}{4}\kappa_{23}a_2^3-\mu pa_1e^{i(\alpha_1-\alpha_2)}-\frac{q}{2}\mu a_1e^{-i(\alpha_1+\alpha_2)}+\frac{q}{2}\mu a_2e^{-2i\alpha_2}+2i\zeta_2\omega a_2-\omega^2a_2+\mu pa_2+\kappa_{21}a_2+\frac{4i\sigma_2}{\pi}=0. \tag{26b}$$

Separating the real and imaginary part, which yields the following system of equations:

$$\begin{cases}\frac{q}{2}a_1\cos(2\alpha_1)-\frac{q}{2}a_2\cos(\alpha_2+\alpha_1)+\frac{3}{4}\kappa_{13}a_1^3+\frac{5}{8}\kappa_{15}a_1^5+(1-\omega^2)a_1-pa_2\cos(\alpha_2-\alpha_1)=0,\\ 2\omega\zeta_1a_1-pa_2\sin(\alpha_2-\alpha_1)-\frac{q}{2}a_1\sin(2\alpha_1)+\frac{q}{2}a_2\sin(\alpha_2+\alpha_1)+\frac{4}{\pi}\sigma_1=0\end{cases} \tag{27a}$$

$$\begin{cases}\frac{q}{2}\mu a_2\cos(2\alpha_2)-\frac{q}{2}\mu a_1\cos(\alpha_1+\alpha_2)+\frac{3}{4}\kappa_{23}a_2^3+\frac{5}{8}\kappa_{25}a_2^5+(\kappa_{21}+\mu p-\omega^2)a_2-\mu pa_1\cos(\alpha_1-\alpha_2)=0\\ 2\omega\zeta_2a_2-\mu pa_1\sin(\alpha_1-\alpha_2)-\frac{q}{2}\mu a_2\sin(2\alpha_2)+\frac{q}{2}\mu a_1\sin(\alpha_1+\alpha_2)+\frac{4}{\pi}\sigma_2=0\end{cases} \tag{27b}$$

Note that, Eqs. (27a), (27b) obtained from separating the real and imaginary parts of Eqs. (26a), and (26b), respectively.

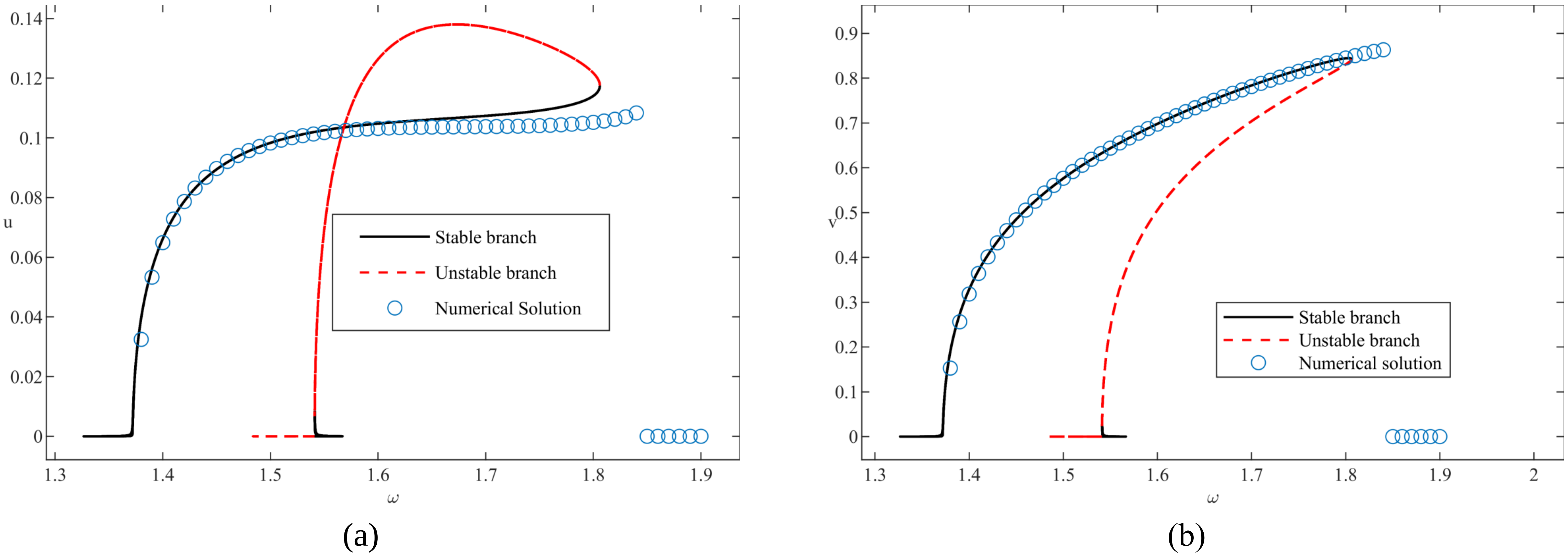

Fig. 10: Branches of periodic orbits (amplitudes), for $m_1 = 4.55$, $m_2 = 9.10$, $\mu = 2$, $\zeta_1 = 0.0423$, $\zeta_2 = 2 * \zeta_1$, $\sigma_1 = 0.0134$, $\sigma_2 = 2*\sigma_1$, $\kappa_{11}= 0.7224$, $\kappa_{13} = 0.3429$, $\kappa_{15} = 1.2910$, $\kappa_{21} = 2*\kappa_{11}$, $\kappa_{23} = 2*\kappa_{13}$, $\kappa_{25} = 2*\kappa_{15}$ obtained using CAM for stiffness characteristics described by a 5th-degree nonlinearity, compared to the numerical solution.

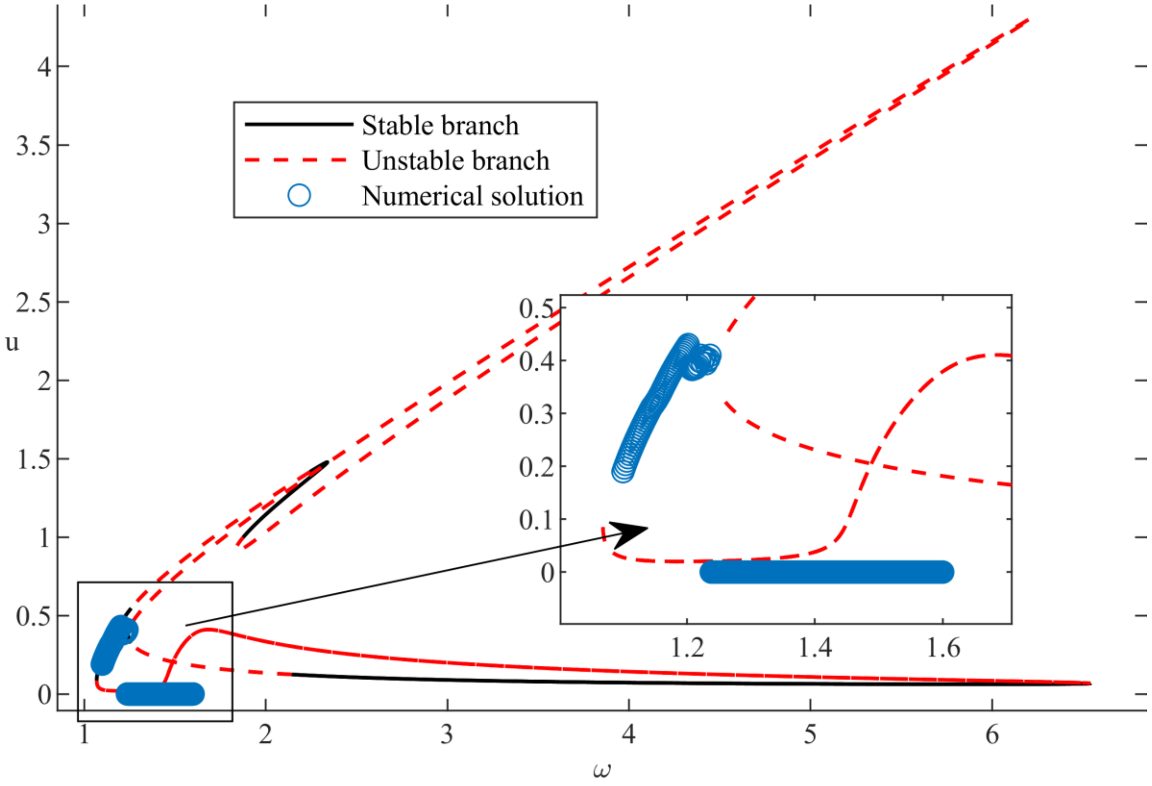

(a)

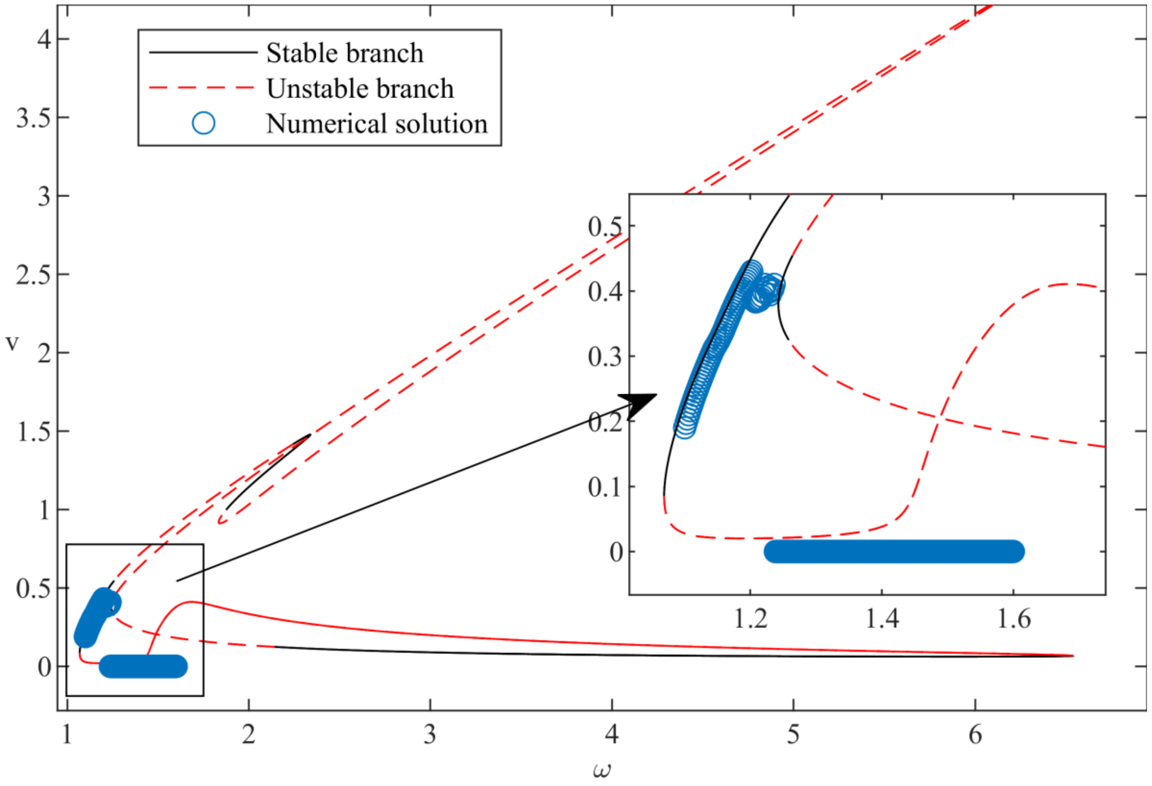

(b)

Fig. 11: Complex branches of periodic orbits (amplitudes), for $\sigma_1 = 0.0134$, $\sigma_2 = 0.0070$, obtained using Complex Averaging Method for stiffness characteristics described by a 5th-degree polynomial, compared to the numerical solution.

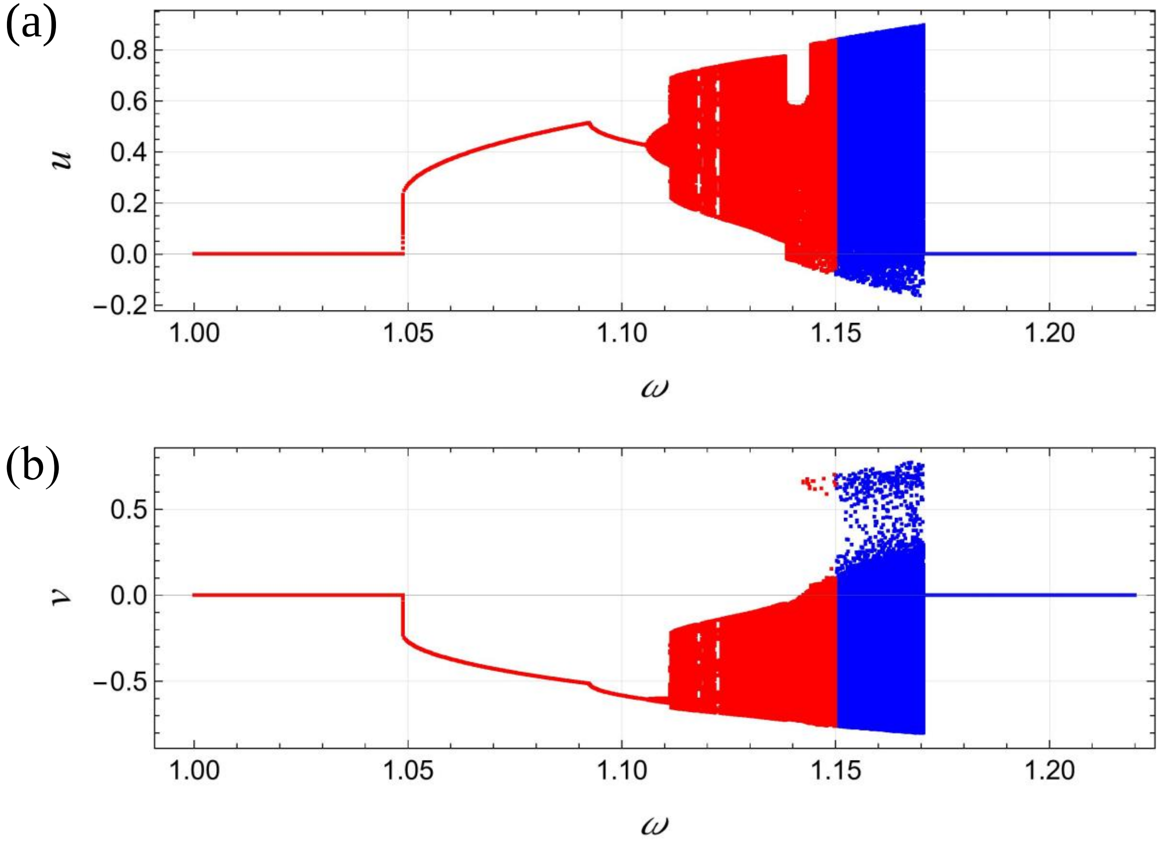

Fig. 12: Bifurcation plot of the local maxima of $u(\tau)$ and $v(\tau)$ as the excitation frequency ω ranges from 1.15 to 1.0 (for backward) 1.15 to 1.22 (for forward) and initial conditions u(0) =0.72, u'(0) = 0.64, v(0)=0.8, and v'(0)=0 for fifth-degree nonlinearity (same masses).

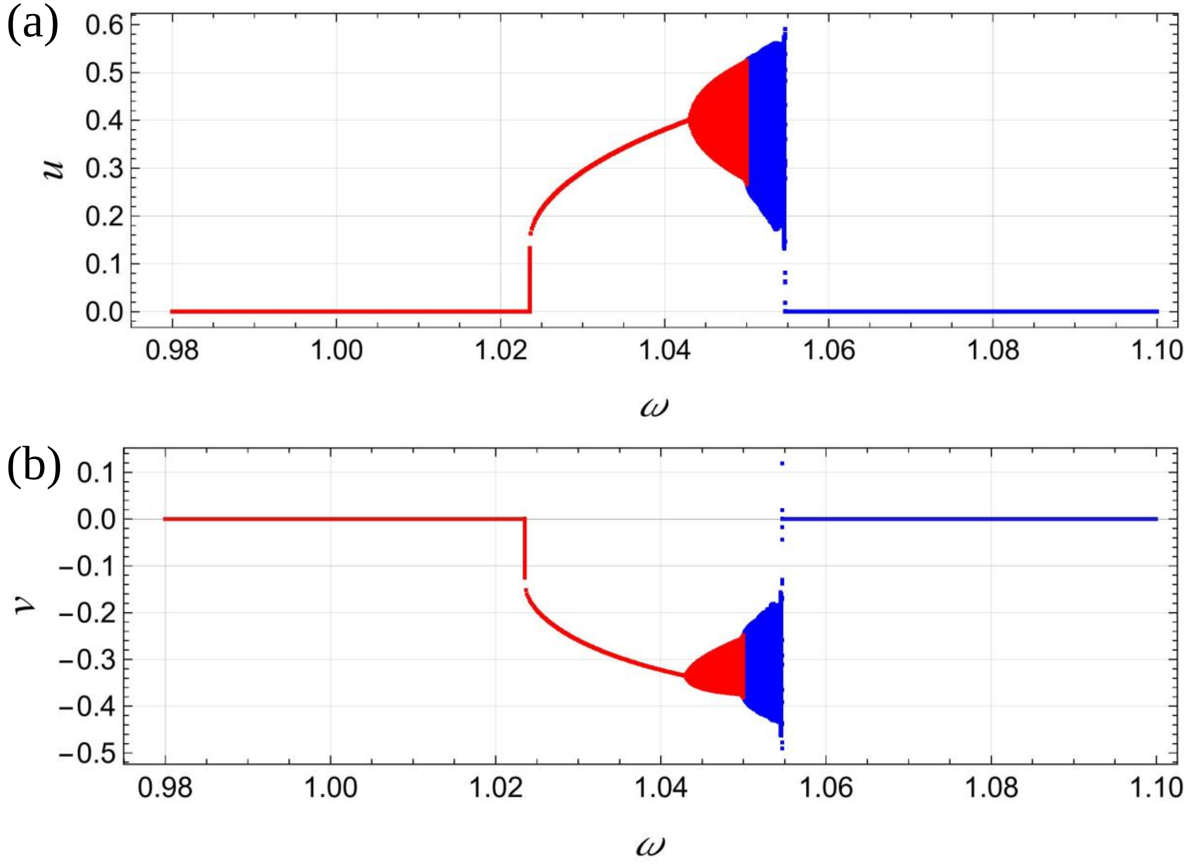

Fig. 13 Bifurcation plot of the local maxima of $u(\tau)$ and $v(\tau)$ as the excitation frequency ω ranges from 1.05 to 0.98 (for backward) 1.05 to 1.10 (for forward) and initial conditions u(0) =0.80, u'(0) = 0.90, v(0) =1.05, and v'(0) =0.05 for fifth-degree nonlinearity (different masses).

The same masses of oscillators

Department of Automation,
Biomechanics and Mechatronics

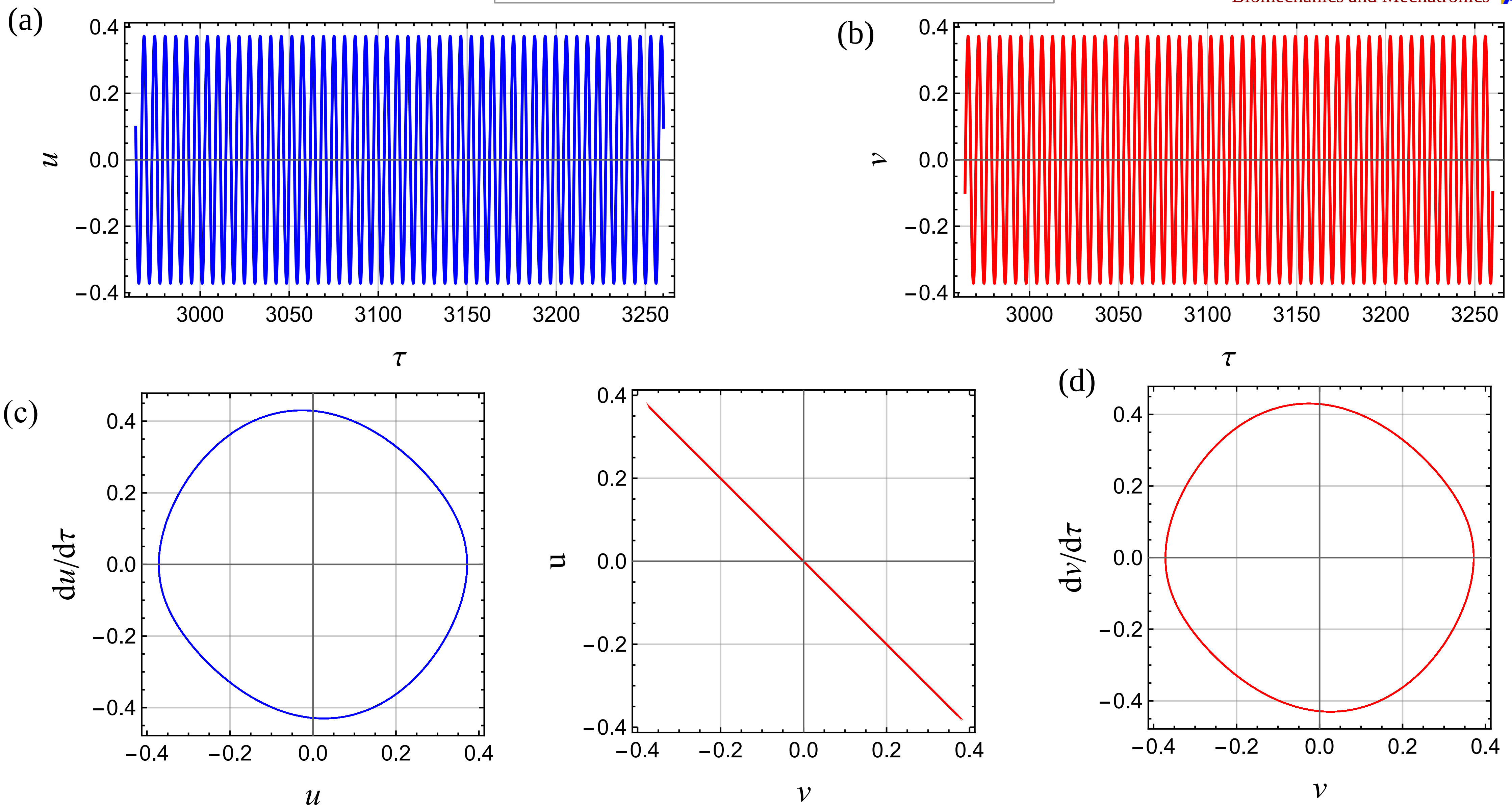

Fig. 14: The time-domain plots (top) show steady-state oscillations for $u(\tau)$ and $v(\tau)$ after an initial transient phase of 500 periods, $\omega = 1.06$, and initial conditions are $u(0) = 0.4$, $u'(0) = 0$, $v(0) = -0.45$, and $v'(0) = 0$. The phase-space plots (bottom) display closed-loop trajectories, indicating periodic, stable motion in antiphase mode.

The same masses of oscillators

Department of Automation,
Biomechanics and Mechatronics

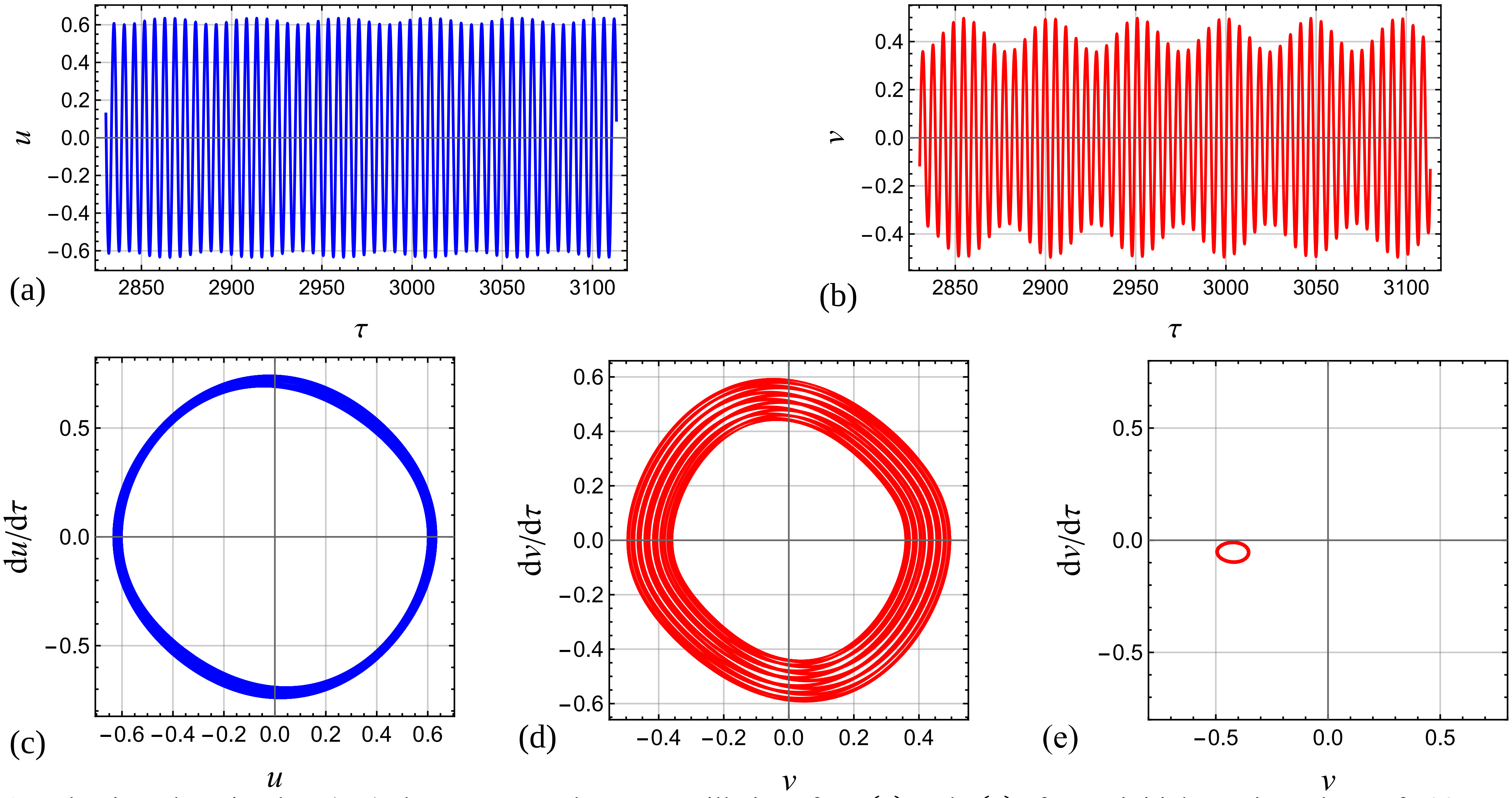

Fig. 15: The time-domain plots (top) show near steady-state oscillations for $u(\tau)$ and $v(\tau)$ after an initial transient phase of 500 periods, $\omega = 1.11$, and initial conditions are $u(0) = 0.4$, $u'(0) = 0$, $v(0) = -0.45$, and $v'(0) = 0$. The phase-space plots (bottom) display closed-loop trajectories, and Poincaré section indicates quasi-periodic motion.

The same masses of oscillators

Department of Automation,
Biomechanics and Mechatronics

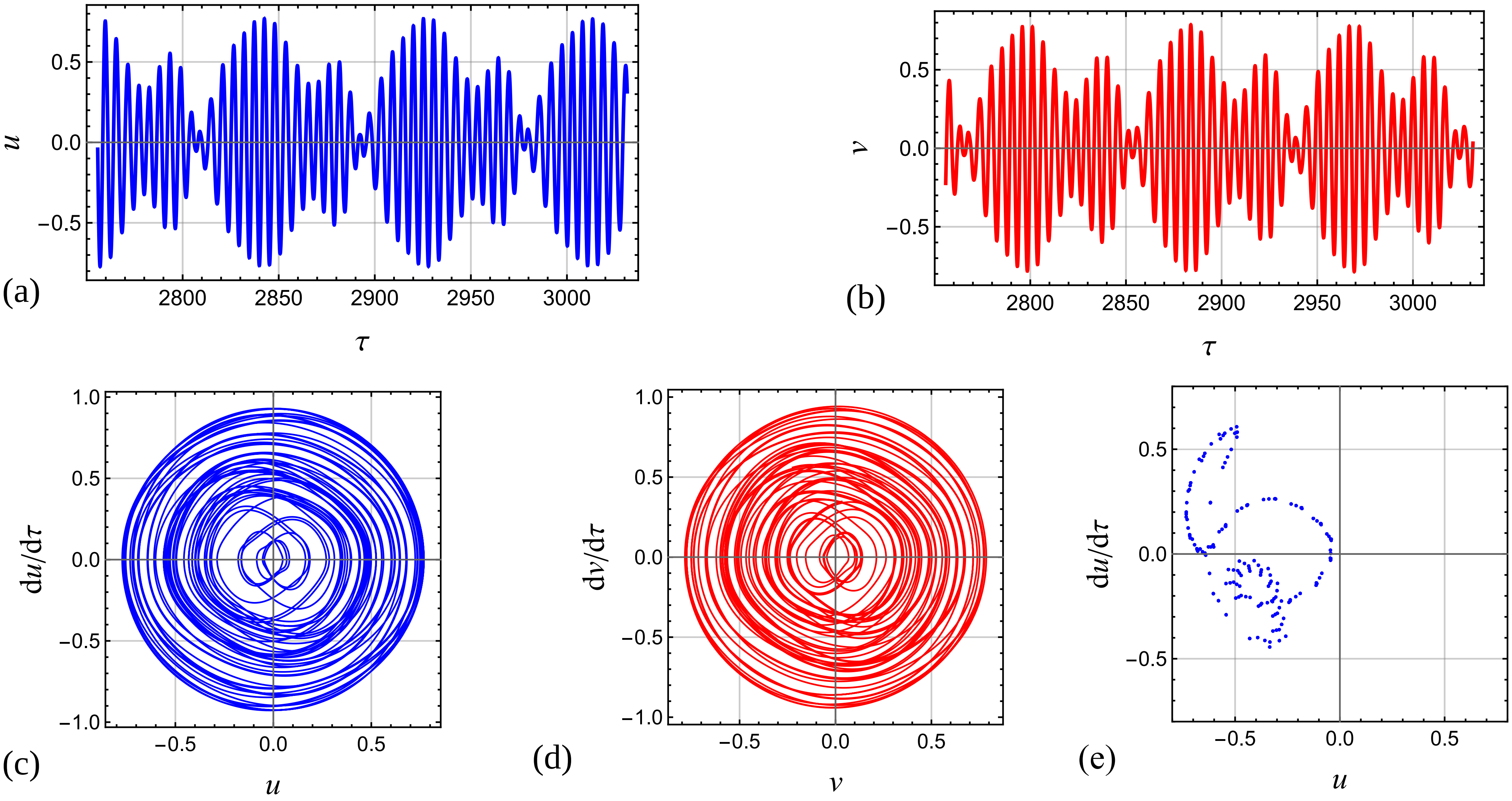

Fig. 12: The time-domain plots (top) show near steady-state oscillations for $u(\tau)$ and $v(\tau)$ after an initial transient phase of 500 periods, $\omega = 1.14$, and initial conditions are $u(0) = 0.4$, $u'(0) = 0$, $v(0) = -0.45$, and $v'(0) = 0$. The phase-space plots (bottom) display uncertain trajectory, and Poincaré section indicates chaotic regime.

The different masses of oscillators

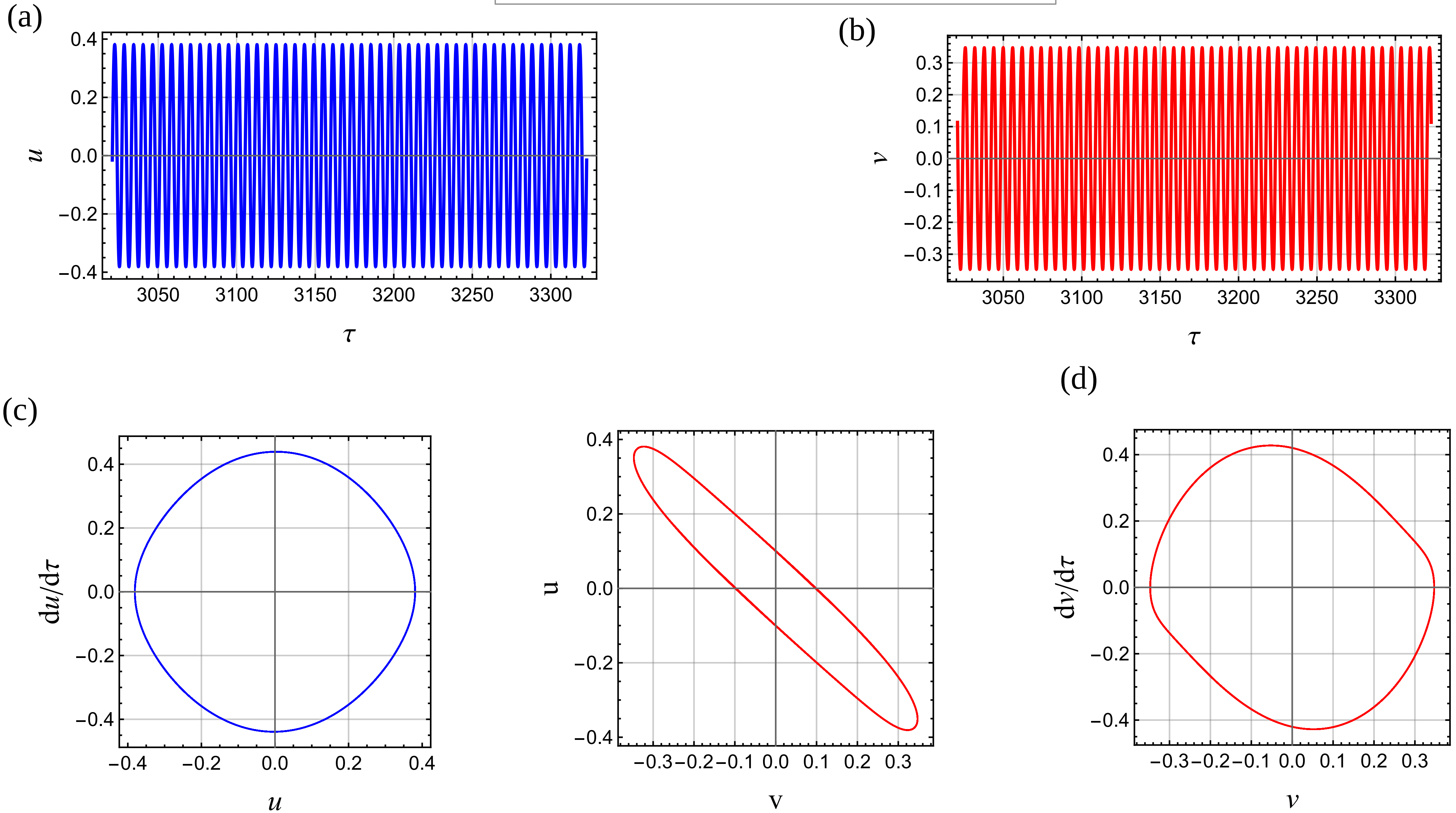

Fig. 12: The time-domain plots (top) show steady-state oscillations for $u(\tau)$ and $v(\tau)$ after an initial transient phase of 500 periods, $\omega = 1.04$, and initial conditions are $u(0) = 0.8$, $u'(0) = 0.9$, $v(0) = 1.05$, and $v'(0) = 0.05$. The phase-space plots (bottom) display closed-loop trajectories, indicating periodic, stable motion in antiphase mode.

The different masses of oscillators

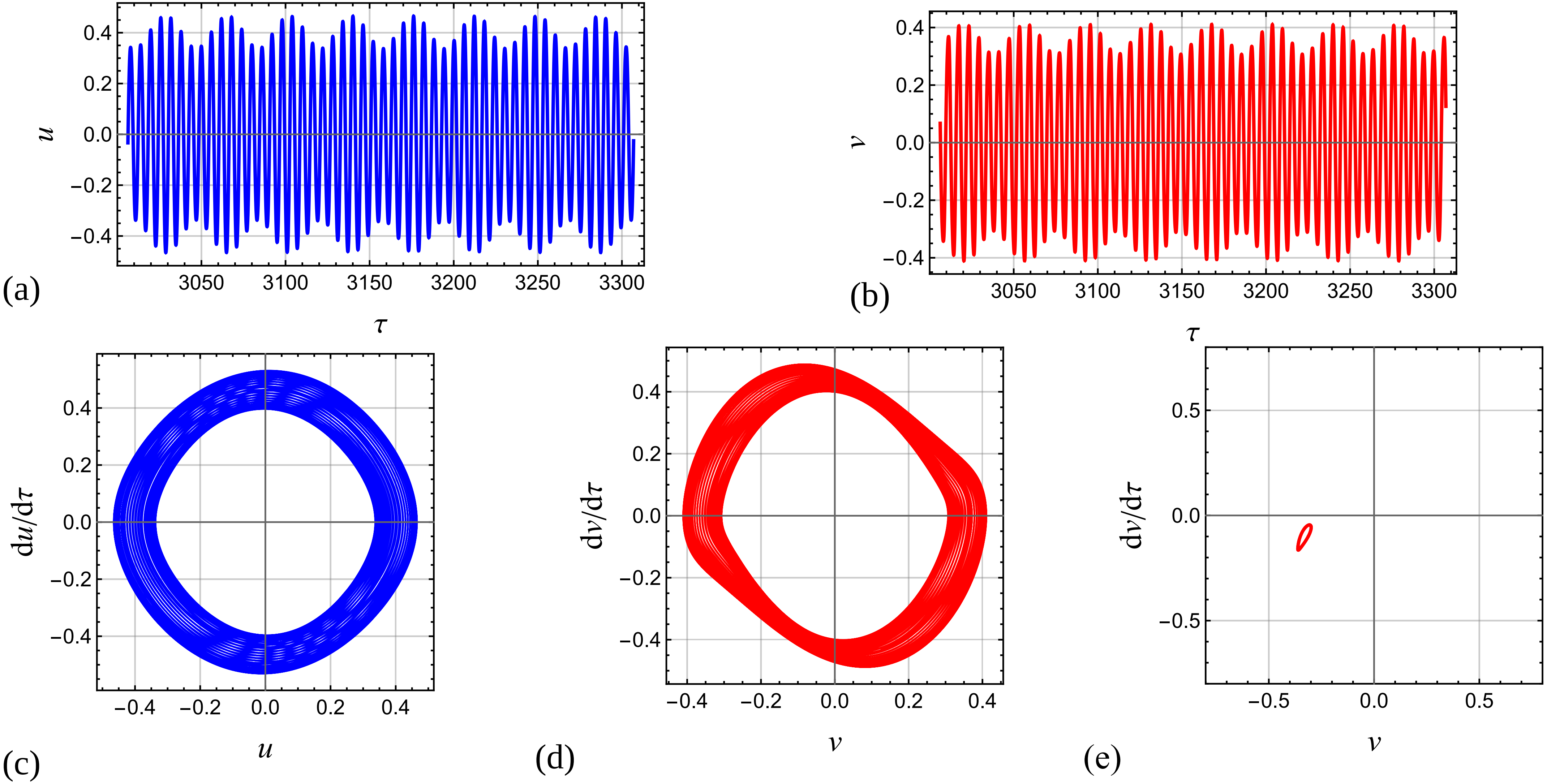

Fig. 12: The time-domain plots (top) show near steady-state oscillations for $u(\tau)$ and $v(\tau)$ after an initial transient phase of 500 periods, $\omega = 1.045$, and initial conditions are $u(0) = 0.8$, $u'(0) = 0.9$, $v(0) = 1.05$, and $v'(0) = 0.05$. The phase-space plots (bottom) display closed-loop trajectories, and Poincaré section indicates quasi-periodic motion.

The different masses of oscillators

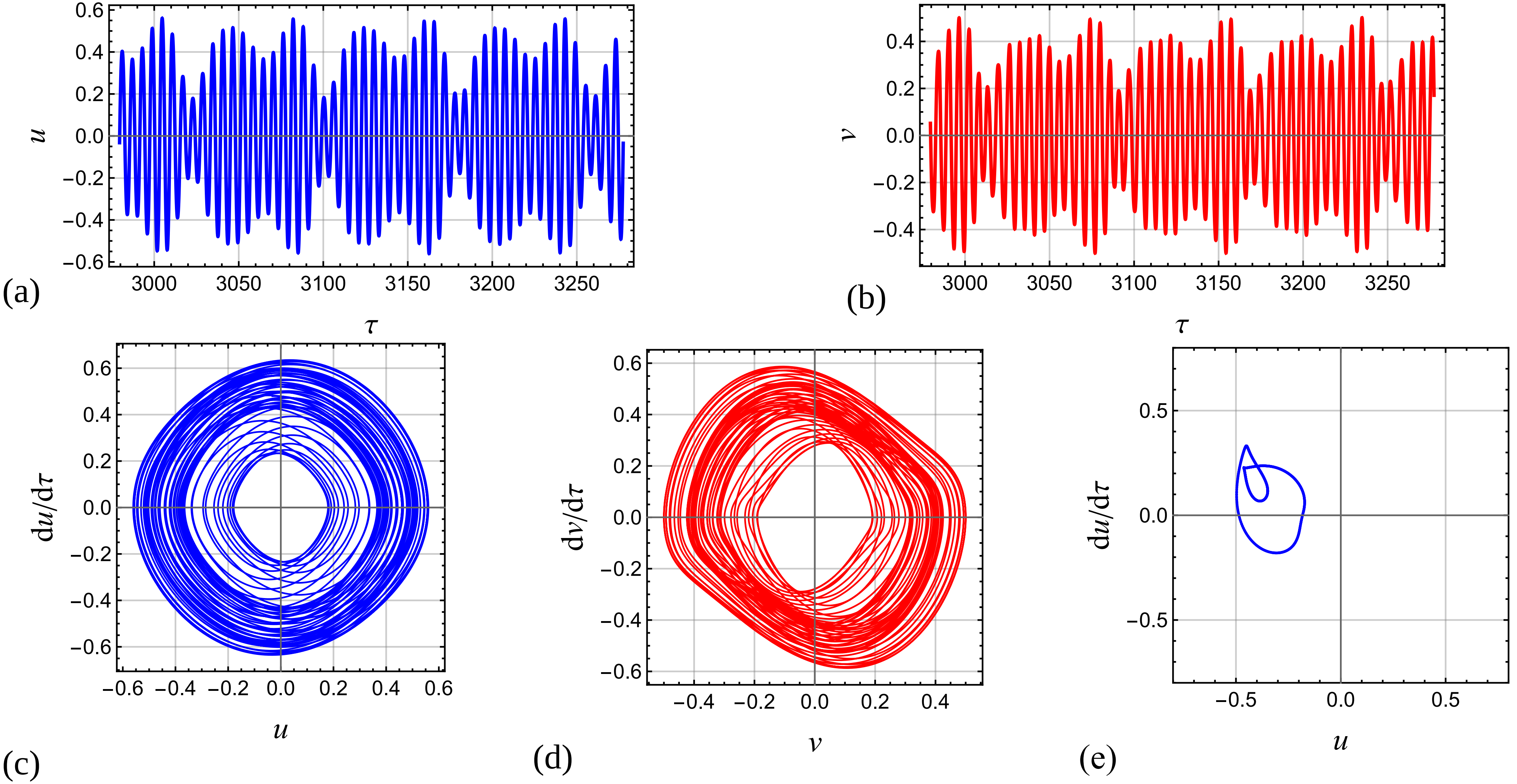

Fig. 12: The time-domain plots (top) show near steady-state oscillations for $u(\tau)$ and $v(\tau)$ after an initial transient phase of 500 periods, ω = 1.0544, and initial conditions are u(0) =0.8, u'(0) = 0.9, v(0) =1.05, and v'(0) =0.05. The phase-space plots (bottom) display closed-loop trajectories, and Poincaré section indicates quasi-periodic motion.

Conclusion

- Investigated 1DOF and 2DOF mechanical parametric oscillators with dry friction.
- Employed analytical methods:
  - (i) Multiple Scale Method (MSM)
  - (ii) Harmonic Balance Method (HBM)
  - (iii) Complex Averaging Method (CAM)
- Explored isolated branches of periodic orbits under nonlinear stiffness and dry friction.
- Analytical solutions (3rd and 5th-degree polynomial approximations) closely matched numerical and experimental results.
- Demonstrated the significance of friction and nonlinearity in system behavior and bifurcation dynamics.
- Validated the effectiveness of proposed models for predicting complex dynamic responses.
- Obtained results support the development of more efficient and controlled mechanical oscillator systems.

References

- G. Kudra, K. Witkowski, A. Fasihi, G. Wasilewski, S. Seth, K. Polczyński, J. Awrejcewicz, Bifurcation dynamics of 1DOF parametric oscillator with stiffness-hardening characteristic and dry friction. Journal of Sound and Vibration, 543-(2023)-117356.
- S. Benacchio, C. Giraud-Audine, O. Thomas, Effect of dry friction on a parametric nonlinear oscillator, Nonlinear Dynam. 108- (2)-(2022)-1005-1026
- K. Witkowski, G. Kudra, S. Skurativskyi, G. Wasilewski, J. Awrejcewicz, Modeling and dynamics analysis of a forced two-degree-of-freedom mechanical oscillator with magnetic springs, Mech. Syst. Signal Process. 148-(2021)-107138.
- S. Seth, G. Kudra, K. Witkowski, J. Awrejcewicz, Equivalent electronic circuit of a system of oscillators connected with periodically variable stiffness, Appl. Sci. 12 (4)-(2022) -2024.
- Awrejcewicz, J., Starosta, R., Sypniewska-Kamińska, G. (2022). Asymptotic Multiple Scale Method in Time Domain: Multi-Degree-of-Freedom Stationary and Nonstationary Dynamics. CRC Press.
- A. H. Nayfeh, Resolving Controversies in the Application of the Method of Multiple Scales and the Generalized Method of Averaging, Nonlinear Dynamics, 40-(2005)-61-102

THANK YOU FOR YOUR ATTENTION